Available online at www.sciencedirect.com
SCIENCE DIRECT®
Physica B 364 (2005) 218–224
PHYSICA B
www.elsevier.com/locate/physb

Thermoelectric properties of Bi-doped Mg_2Si semiconductors

Jun-ichi Tani*, Hiroyasu Kido

Department of Electronic Materials, Osaka Municipal Technical Research Institute, 1-6-50 Morinomiya, Joto-ku, Osaka 536-8553, Japan

Received 25 February 2005; received in revised form 11 April 2005; accepted 11 April 2005

Abstract

The thermoelectric properties of Bi-doped Mg_2Si (Mg_2Si:Bi = 1:x) fabricated by spark plasma sintering process have been characterized by Hall effect measurements at 300 K and by measurements of electrical resistivity (ρ), Seebeck coefficient (S), and thermal conductivity (κ) between 300 and 900 K. Bi-doped Mg_2Si samples are n-type in the measured temperature range. The electron concentration of Bi-doped Mg_2Si at 300 K ranges from $1.8 \times 10^{19}\,cm^{-3}$ for the Bi concentration $x = 0.001$ to $1.1 \times 10^{20}\,cm^{-3}$ for $x = 0.02$. The solubility limit of Bi in Mg_2Si is estimated to be about 1.3 at% and first-principles calculation revealed that Bi atoms are expected to be primarily located at the Si sites in Mg_2Si. The electrical resistivity, Seebeck coefficient, and thermal conductivity are strongly affected by the Bi concentration. The sample of $x = 0.02$ shows a maximum value of the figure of merit, ZT, is 0.86 at 862 K.

PACS: 72.20.Pa; 71.55.−i

Keywords: Semiconductor; Thermoelectric material; Hall effect; Mg_2Si; First-principles calculation

1. Introduction

The intermetallic compounds such as Mg_2X (X = Si, Ge, Sn) and their solid solutions are semiconductors having the antifluorite structure and have been proposed to be good candidates for high-performance thermoelectric materials, because of their superior features such as its large Seebeck coefficient, low electrical resistivity, and low thermal conductivity [1–4]. There have been some attempts to dope additives into Mg_2(Si, Ge, Sn) to control its semiconducting properties. The conduction types are p-type, produced by doping with Ag and Cu and n-type, produced by doping with Sb and Al [2–7].

For thermoelectric materials, a large Seebeck coefficient, S, a small electrical resistivity, ρ, and a small thermal conductivity, κ, are required. These quantities determine the so-called thermoelectric figure of merit, $Z = S^2/\rho\kappa$. A low lattice thermal conductivity and a high carrier mobility are desirable for improvement of the figure of merit.

*Corresponding author. Tel.: +81 6 6963 8081; fax: +81 6 6963 8099.
E-mail address: tani@omtri.city.osaka.jp (J. Tani).

0921-4526/$ - see front matter © 2005 Elsevier B.V. All rights reserved.
doi:10.1016/j.physb.2005.04.017

Vining [8] pointed out that a factor $A' = (T/300)(m^*/m_e)^{3/2} m\kappa_{ph}$, where m^* is the carrier effective mass, m is the mobility in $cm^2/V\,s$, and κ_{ph} is the lattice thermal conductivity in mW/cmK, is a larger value of 3.7–14 for Mg_2(Si, Ge, Sn), as compared with 1.2–2.6 for SiGe and 0.05–0.8 for β-$FeSi_2$ and therefore Mg_2(Si, Ge, Sn) system will achieve higher ZT with further development.

Recently, Kajikawa et al. [9,10] and Umemoto et al. [11] reported thermoelectric properties of Mg_2Si fabricated by spark plasma sintering (SPS), which is a novel process because it is reported that the diffusion velocity becomes extremely large even at low temperatures due to pulse electric field superposed on DC. In case of Mg_2Si, SPS plays two roles: (a) solid-state reaction process between Mg and Si, (b) densification process in a short time at relatively low temperatures, which would be effective to suppress the volatilization of Mg as well as dopants with low melting point. Bi has a low melting point of 545 K [12] and belongs to same Vb group as Sb, which is n-type dopant of Mg_2Si. For Bi-doped Mg_2Si, a low thermal conductivity might be possible because Bi has a larger radius than other n-type dopants such as Al and Sb. However, to our knowledge, there has been no research concerning the thermoelectric properties of Bi-doped Mg_2Si.

In this paper, the thermoelectric properties of Bi-doped Mg_2Si fabricated by SPS process have been characterized by Hall effect measurements at 300 K and by measurements of electrical resistivity, Seebeck coefficient, and thermal conductivity between 300 and 900 K. Finally, an optimum composition giving the largest ZT value in the present system is determined. We have also performed quantum-mechanical first-principles calculations of Bi-doped Mg_2Si within density functional theory to obtain information on the preferential site occupation of Bi in Mg_2Si.

2. Experiment and details of the calculations

Powders of high purity, Mg (>99.9%), Si (>99.999%), and Bi (>99.9%), were used as starting materials. The Mg and Si were mixed in 2:1 ratio and varying an amount of Bi (the molar ratio of $Mg_2Si{:}Bi = 1{:}x$) were added to each charge. They were ground together, and then heated in a graphite die (15 mm in diameter) at 1023–1053 K for 15 min at 30 MPa under a vacuum of 1×10^{-3} Torr by the SPS method with a heating rate of 60 K/min. The density of the annealed samples was more than 99% of the theoretical value.

X-ray diffraction by Cu Kα radiation of the samples detected only the anti-fluorite type structure. The Hall coefficient (R_H) was measured for 1.5-cm-diameter, 0.1-cm-thick samples using the Toyo Corporation Resitest 8320. The contacts between the samples and lead Au wires were formed by soldering with In. The Hall effect was measured at 300 K using an alternating current (AC) magnetic method, under an applied magnetic field of 0.39 T at a frequency of 200 mHz. The carrier concentration (n) of the samples was determined by the factor $1/e|R_H|$. The Seebeck coefficient (S) was measured by the standard technique using Pt electrodes in a He gas atmosphere in the temperature range of 300–900 K using an ULVAC ZEM-1S. The temperature gradient across the length of the sample was about 5 K. The electrical resistivity (ρ) was also measured concurrently by the four-probe DC method. The thermal diffusion coefficients of the samples were measured by the conventional laser flash method using a thermal constant analyzer (ULVAC TC-7000). The disk specimen was set in an electric furnace and heated to 900 K under vacuum. After the temperature was stabilized, the front surface of the specimen was irradiated by a ruby laser pulse. The temperature variation at the surface was monitored with a Pt–Pt 13%Rh thermocouple and an InSb infrared detector. The density was measured by the Archimedes method. The thermal conductivity was calculated from the experimental thermal diffusivity as well as density values and a previous reported specific heat capacity data of nondoped Mg_2Si investigated by Riffel and Schilz [13].

In order to investigate geometrical structure of Bi-doped Mg_2Si, density functional theory (DFT) calculations within the pseudopotential and generalized gradient approximations (GGAs) were performed using the computer program CASTEP

(Cambridge Serial Total Energy Package in Cerius2, Accelrys Inc.) [14]. We constructed a supercell containing 48 atoms ($Mg_{32}Si_{16}$) with the space group $Fm\bar{3}m$ and replaced one of the 48 sites of the Mg or Si atoms by Bi. We expanded the valence electronic wave functions in a plane-wave basis set up to an energy cutoff of 400 eV, which converges the total energy of the unit cell to better than 1 meV/atom. The Brillouin zone integrations were preformed at the Γ point for the 48-atom unit cell. The electron–ion interaction is described by a Vanderbilt's ultrasoft pseudopotentials [15]. The lattice constant was determined through calculations for the primitive cell, using a plane-wave cutoff energy of 400 eV and the calculated value is 99.9% of the experimental value reported for Mg_2Si [16]. The positions of the atoms within the second nearest neighbors of the impurity were allowed to relax under a constant volume condition by total energy minimization, until the residual forces for the relaxed atoms were $<0.1\,eV/Å$.

3. Results and discussion

Table 1 lists the results of the Hall effect and electrical resistivity measurements at 300 K of Bi-doped Mg_2Si, compared to those of nondoped Mg_2Si. The sign for R_H of nondoped and Bi-doped Mg_2Si is negative, indicating that the conductivity is mainly due to electrons. The Hall mobility ($m_H = R_H/\rho$) at 300 K of Bi-doped Mg_2Si is lower than the value 204 $cm^2/V\,s$ of nondoped Mg_2Si. m_H of Bi-doped Mg_2Si shows composition dependence and shows the highest value of 92.4 $cm^2/V\,s$ at $x = 0.005$ in the composition range $0.001 \leqq x \leqq 0.02$. The m_H of Bi-doped Mg_2Si is larger than the reported values 41.5 $cm^2/V\,s$ for 0.6 mol% Sb-doped Mg_2Si investigated by Kajikawa [9]. The carrier concentration of nondoped Mg_2Si is $4.3 \times 10^{17}\,cm^{-3}$, while that of Bi-doped Mg_2Si is $1.8 \times 10^{19}\,cm^{-3}$ for $x = 0.001$ to $1.1 \times 10^{20}\,cm^{-3}$ for $x = 0.02$. In the Bi-doped Mg_2Si, the carrier concentration is almost proportional to the doping concentration within the composition range of $0.000 \leqq x \leqq 0.01$. If Bi atom is soluble in Mg_2Si, carrier concentration should correspond to the Bi atom concentration. Therefore, a solid solution of Bi-doped Mg_2Si exists at least in the range of $0.000 \leqq x \leqq 0.01$. However, the carrier concentration for $x = 0.02$ is much lower than a value from a straight line in Fig. 1. This fact suggests that Bi atoms are not completely soluble for $x = 0.02$. From the plot in Fig. 1, the solubility limit is estimated to be 1.3 at%.

There is no information on the preferential site occupation of Bi in Mg_2Si. So, we performed quantum-mechanical first-principles calculations of Bi-doped Mg_2Si within density functional theory to obtain information on the preferential site occupation of Bi in Mg_2Si.

$$Mg_{32}Si_{16} + Bi \rightarrow Mg_{31}Si_{16}Bi + Mg, \quad (1)$$

$$Mg_{32}Si_{16} + Bi \rightarrow Mg_{32}Si_{15}Bi + Si. \quad (2)$$

The energetic difference between reactions (1) and (2) is estimated:

$$\Delta E_t = \{E_t(Mg_{31}Si_{16}Bi) + \mu_{Mg}\} - \{E_t(Mg_{32}Si_{15}Bi) + m_{Si}\}. \quad (3)$$

Table 1
Electrical properties of Bi-doped Mg_2Si (Mg_2Si: Bi = 1:x ($0.000 \leqq x \leqq 0.020$)) at 300 K

x (at%)	Conduction type	Carrier concentration (cm^{-3})	Mobility ($cm^2/V\,s$)	Resistivity (Ωcm)
0.0	N	4.3×10^{17}	204	7.14×10^{-2}
0.1	N	1.8×10^{19}	85.7	3.97×10^{-3}
0.3	N	3.1×10^{19}	91.5	2.22×10^{-3}
0.5	N	4.1×10^{19}	92.4	1.64×10^{-3}
1	N	8.5×10^{19}	63.5	1.16×10^{-3}
2	N	1.1×10^{20}	64.0	8.58×10^{-4}

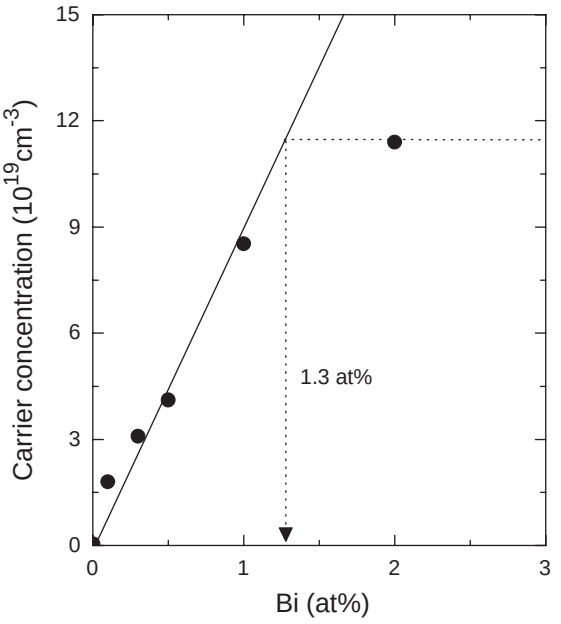

Fig. 1. Bi atom concentration (x) dependence of carrier concentration (n) of Bi-doped Mg_2Si at 300 K.

The chemical potentials of m_{Mg} and m_{Si} can be varied within a range limited by the three constraints:

$$m_{Mg} \leqq m_{Mg}\,(\text{bulk}), \tag{4}$$

$$m_{Si} \leqq m_{Si}\,(\text{bulk}), \tag{5}$$

$$2m_{Mg} + m_{Si} = m_{Mg_2Si}\,(\text{bulk}), \tag{6}$$

where m_{Mg_2Si} (bulk), the chemical potential of the bulk Mg_2Si, is a constant value calculated as the total energy per Mg_2Si unit formula. The formation energies were calculated under the two extreme conditions, the Si-rich limit ($m_{Mg} = 1/2(m_{Mg_2Si\,(bulk)} - m_{Si\,(bulk)})$ and $m_{Si} = m_{Si\,(bulk)}$) and the Mg-rich limit ($m_{Si} = m_{Mg_2Si\,(bulk)} - 2m_{Mg\,(bulk)}$ and $m_{Mg} = m_{Mg\,(bulk)}$). The calculated total energies of the Mg_2Si perfect crystal, the Bi-doped crystals, Si atom calculated from the Si crystal (space group $Fd\bar{3}m$, cubic structure), and Mg atom calculated from the Mg crystal (space group $P6_3/mmc$, hexagonal structure) are shown in Table 2. A comparison of the computed total energies revealed that ΔE_t is 1.25 and 2.06 eV at the Si-rich and Mg-rich limit, respectively. Therefore, the substitution at the Si sites is lower than that for substitution at the Mg sites. Therefore, Bi atoms are expected to be primarily located at the Si sites in Mg_2Si. The n-type conduction can be interpreted as a result indicating that Bi atoms (Vb group) in Mg_2Si are substituted by Si atoms (IVb group) and act as donors. Kajikawa et al. [9] reported that Sb is estimated to be replaced to Si site from the results of electron probe microanalysis (EPMA). Taking into account that Bi is the same group Vb as Sb and Sb-doped Mg_2Si shows same n-type behavior, this calculation result seems reasonable.

Table 2
The calculated total energies of Mg_2Si perfect crystal, the Bi-doped crystals, Si atom calculated from the Si crystal, and Mg atom calculated from the Mg crystal

Models	Total energy (eV)
Mg_2Si	−2066.309
$Mg_{31}BiSi_{16}$	−32234.84
$Mg_{32}Si_{15}Bi$	−33106.15
Mg	−978.519
Si	−108.728

Fig. 2 shows the temperature dependence of the electrical resistivity (ρ) of Bi-doped Mg_2Si, as compared with that of nondoped Mg_2Si. ρ of Bi-doped Mg_2Si decreases with increasing x. ρ of Bi-doped Mg_2Si has an almost constant value at 300–380 K, but increases gradually with increasing temperature at 380–900 K. LaBotz et al. [1] and Noda et al. [4] reported that the temperature dependence of mobility in $Mg_2Si_xGe_{1-x}$ indicates $m \propto T^{-3/2}$ and the acoustic lattice scattering is the predominant mechanism. Therefore, the increment of ρ at 380–900 K will be explained by the decrease of mobility with increasing temperature. On the other hand, the ρ of nondoped Mg_2Si increases, reaching a maximum at 470 K, and then decrease with increasing temperature. The decrease of ρ at high temperatures is explained by a result that the intrinsic conduction will occur due to the band gap of 0.77 eV [17,18].

Fig. 3 shows the temperature dependence of the Seebeck coefficient (S) of Bi-doped Mg_2Si,

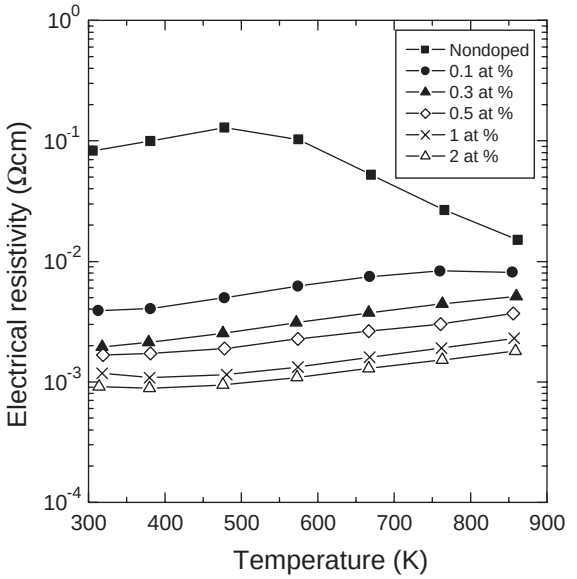

Fig. 2. Electrical resistivity (ρ) of Bi-doped Mg_2Si (Mg_2Si:Bi = 1:x ($0.001 \leqq x \leqq 0.020$)) and nondoped Mg_2Si as a function of temperature.

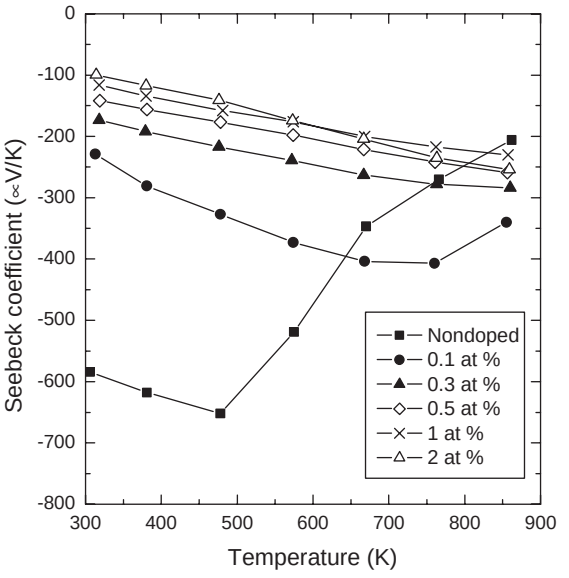

Fig. 3. Seebeck coefficient (S) of Bi-doped Mg_2Si (Mg_2Si:Bi = 1:x ($0.001 \leqq x \leqq 0.020$)) and nondoped Mg_2Si as a function of temperature.

as compared with that of nondoped Mg_2Si. The polarity of S for Bi-doped Mg_2Si is negative, indicating that the conductivity is mainly due to electrons. At 300 K, the polarity of S is in good agreement with the sign of R_H, and the absolute value of S corresponds to the value of electron concentration. The absolute S for $x = 0.003$, 0.005, 0.01 and 0.02 increases with increasing temperature. The absolute S of nondoped Mg_2Si as well as $x = 0.001$, however, increases, reaching a maximum at 470 and 750 K, respectively and then decrease with increasing temperature.

Fig. 4 shows the temperature dependence of thermal conductivity (κ) of Bi-doped Mg_2Si, as compared with that of nondoped Mg_2Si. κ decreases with increasing temperature at 300–660 K, and shows a almost constant value above 660 K. At low temperatures, κ depends strongly on x and decreases with increasing x. The κ is the sum of the contributions arising from the lattice (κ_{ph}), and the electronic (κ_{el}) components. In order to understand the thermal conductivity behavior of Bi-doped Mg_2Si, it is necessary to determine the temperature and composition

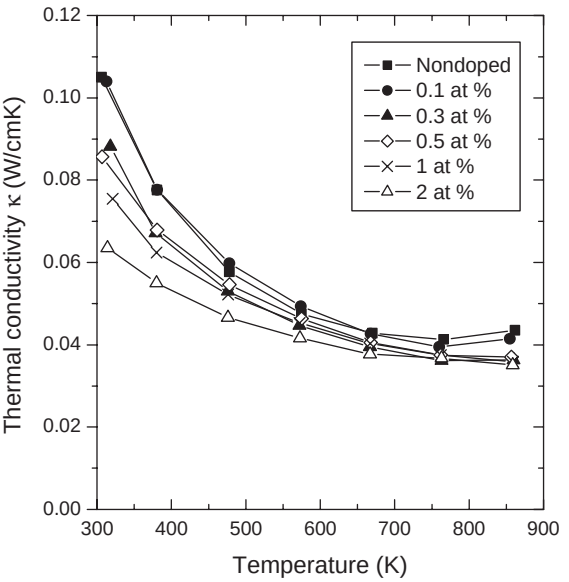

Fig. 4. Thermal conductivity (κ) of Bi-doped Mg_2Si (Mg_2Si:Bi = 1:x ($0.001 \leqq x \leqq 0.020$)) and nondoped Mg_2Si as a function of temperature.

dependences of κ_{ph} and κ_{el}. We can calculate κ_{el} using the Wiedemann–Franz law [19], $\kappa_{el} = L_0 \sigma T$ (L_0, Lorentz number $2.45 \times 10^{-8}\,V^2/K^2$, σ,

electrical conductivity, T, absolute temperature). It is possible to calculate κ_{ph} by subtracting κ_{el} from κ.

Fig. 5 shows the temperature dependence of κ_{ph} and κ_{el} in the thermal conductivity of Bi-doped Mg_2Si and nondoped Mg_2Si. κ_{ph} decreases with an increase in x and temperature. However, κ_{el} increases with an increase in x and temperature. For $x = 0.001$, the ratio of κ_{el} to κ_{ph} at 300 K is about 1/50, and it is about 1/15 at 860 K. For $x = 0.02$, the ratio of κ_{el} to κ_{ph} at 300 K is about 2/13, and it is about 1/2 at 860 K. Therefore, the thermal conductivity of Bi-doped Mg_2Si is mainly influenced by κ_{ph}. The κ_{ph} of Bi-doped Mg_2Si and nondoped Mg_2Si is proportional to T^{-1}, indicating that phonon–phonon interactions are the primary source of thermal resistance. This mechanism is in good agreement with an early work of nondoped Mg_2Si investigated by LaBotz and Mason [20].

Fig. 6 shows the temperature dependence of ZT of Bi-doped Mg_2Si, as compared with that of nondoped Mg_2Si. The value of ZT increases with increasing temperature. An optimum composition giving maximum ZT value in the present system is $x = 0.02$. The value of Bi-doped Mg_2Si is 0.86 at 862 K, which is 1.5 times larger than an earlier result ($ZT = 0.57$ at 856 K) reported for Al-doped Mg_2Si by Umemoto et al. [14]. In case of Al-doped Mg_2Si, the solubility limit of Al in Mg_2Si is around 0.15 at%, which is much lower than the solubility limit of 1.3 at% of Bi in Mg_2Si and the carrier concentration of 0.1 at. % Al-doped sample is reported to be $1.4 \times 10^{19}\,cm^{-3}$ at room temperature, which is one magnitude lower than Bi-doped Mg_2Si. Therefore, the reason why the higher ZT is

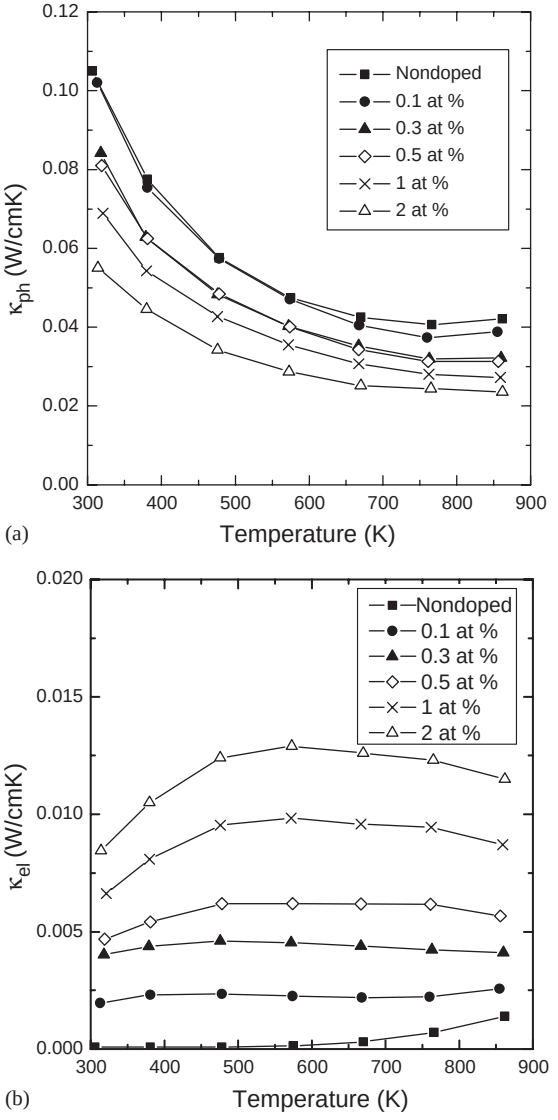

Fig. 5. Carrier contribution (κ_{el}) and lattice contribution (κ_{ph}) in the thermal conductivity of Bi-doped Mg_2Si (Mg_2Si:Bi = 1:x ($0.001 \leqq x \leqq 0.020$)) and nondoped Mg_2Si.

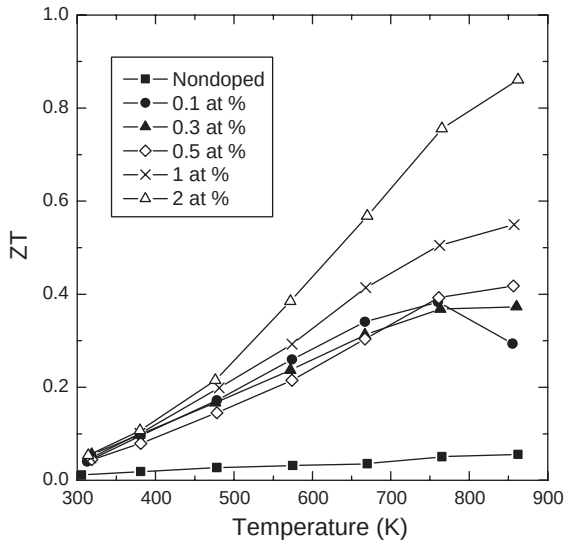

Fig. 6. Dimensionless figure of merit (ZT) of Bi-doped Mg_2Si (Mg_2Si:Bi = 1:x ($0.001 \leqq x \leqq 0.020$)) and nondoped Mg_2Si as a function of temperature.

achieved in Bi-doped Mg_2Si will be explained as a result that the high carrier concentration is obtained because of higher solubility limit of Bi in Mg_2Si.

4. Conclusions

The thermoelectric properties of Bi-doped Mg_2Si fabricated by the spark plasma sintering process have been characterized by Hall effect measurements at 300 K and by measurements of electrical resistivity, Seebeck coefficient, and thermal conductivity between 300 and 900 K. Bi-doped Mg_2Si samples are n-type in the measured temperature range. The electron concentration of Bi-doped Mg_2Si at 300 K ranges from $1.8 \times 10^{19}\,cm^{-3}$ for the Bi concentration $x = 0.001$ to $1.1 \times 10^{20}\,cm^{-3}$ for $x = 0.02$. The solubility limit of Bi in Mg_2Si is estimated to be about 1.3 at% and first-principles calculation revealed that Bi atoms are expected to be primarily located at the Si sites in Mg_2Si. The electrical resistivity, Seebeck coefficient, and thermal conductivity are strongly affected by the Bi concentration. The sample of $x = 0.02$ shows a maximum value of ZT is 0.86 at 862 K, which is 1.5 times larger than an earlier result ($ZT = 0.57$ at 856 K) reported for Al-doped Mg_2Si. Therefore, Bi-doped Mg_2Si is a good candidate material for thermoelectric conversion in the middle-temperature range.

References

[1] R.J. LaBotz, D.R. Mason, D.F. O'Kane, J. Electrochem. Soc. 110 (1963) 127.
[2] E.N. Nikitin, V.G. Bazanov, V.I. Tarasov, Sov. Phys. Solid State 3 (1962) 2648.
[3] Y. Noda, H. Kon, Y. Furukawa, N. Otsuka, I.A. Nishida, K. Masumoto, Mater. Trans. JIM 33 (1992) 845.
[4] Y. Noda, H. Kon, Y. Furukawa, N. Otsuka, I.A. Nishida, K. Masumoto, Mater. Trans. JIM 33 (1992) 851.
[5] R.G. Morris, R.D. Redin, G.C. Danielson, Phys. Rev. 109 (1958) 1909.
[6] R.G. Morris, R.D. Redin, G.C. Danielson, Phys. Rev. 109 (1958) 1916.
[7] M.W. Heller, G.C. Danielson, J. Phys. Chem. Solids 23 (1962) 601.
[8] D.M. Rowe, CRC Handbook of Thermoelectrics, CRC Press, New York, 1995, p. 277.
[9] T. Kajikawa, K. Shida, S. Sugihara, M. Ohmori, T. Hirai, Proceedings of the 16th International Conference on Thermoelectrics (ICT'97), IEEE, 1997, p. 275.
[10] T. Kajikawa, K. Shida, K. Shiraishi, T. Ito, M. Ohmori, T. Hirai, Proceedings of the 17th International Conference on Thermoelectrics (ICT'98), IEEE, 1998, p. 362.
[11] M. Umemoto, Y. Shirai, K. Tsuchiya, Proceedings of the Fourth Pacific Rim International Conference on Advanced Materials and Processing (PRICM4), The Japan Institute of Metals, 2001, p. 2145.
[12] D.R. Lide, CRC Handbook of Chemistry and Physics, 84th ed., CRC Press, New York, 2003, pp. 4–132.
[13] M. Riffel, J. Schilz, Proceedings of the 16th International Conference on Thermoelectrics (ICT'97), IEEE, 1997, p. 283.
[14] CASTEP Users Guide, Accelrys Inc., San Diego, CA, 2001.
[15] D. Vanderbilt, Phys. Rev. B 41 (1990) 892.
[16] J.G. Barlock, L.F. Mondolfo, Z. Metall. 66 (1975) 605.
[17] G. Busch, U. Winkler, Helv. Phys. Acta 26 (1953) 359.
[18] G. Busch, U. Winkler, Physica 20 (1954) 1067.
[19] See, for example, N. W. Ashcroft, N. D. Mermin, Solid State Physics, Holt, Rinehart, & Winston, New York, 1976, p. 20, and references therein.
[20] R.J. LaBotz, D.R. Mason, J. Electrochem. Soc. 110 (1963) 121.